NJC

PAPER

View Article Online
View Journal

Cite this: DOI: 10.1039/c7nj03999a

Serine- and threonine-derived diamine equivalents for site-specific incorporation of platinum centers in peptides, and the anticancer potential of these conjugates†

Sateeshkumar Kumbhakonam,‡[a] Kasipandi Vellaisamy,‡[a] Soumya Saroj,[a] Nalini Venkatesan,[b] Karunagaran D.[b] and Muraleedharan Kannoth Manheri*[a]

Received 17th October 2017,
Accepted 5th January 2018

DOI: 10.1039/c7nj03999a

rsc.li/njc

A modular strategy that allows introduction of one or more reactive platinum units at chosen locations along a peptide sequence is presented. This makes use of diazides generated from serine and threonine as diamine equivalents which can be conjugated to the peptide under standard coupling conditions. Reduction of these diazides using Pd/C and H_2 followed by platination affords the final products in good yields. Following this, we prepared a new class of peptide–platinum conjugates and carried out preliminary cytotoxicity evaluation and DNA interaction studies. Inclusion of lysine residues in the sequence was found to improve DNA interaction and anticancer activities compared to analogous conjugates with hydrophobic side chains.

Introduction

Cisplatin exemplifies the relevance of metal complexes in therapy and is widely used for the treatment of testicular-, ovarian-, head and neck-, bladder-, and cervical cancers. Its dose-limiting toxicity is a concern which reduces the success rates in many cases, especially in the event of resistance.[1–4] Its analogs namely, carboplatin and oxaliplatin, offer some advantage in terms of toxicity, which have also been introduced for treatment worldwide; newer members of this series like nedaplatin, lobaplatin, and heptaplatin at the same time are approved only in specific countries.[5,6] After cellular activation, they are known to cross-link DNA, predominantly through N-7 of guanine. Efforts towards exploring the therapeutic utility of other metal complexes have led to the identification of a number of leads from Ru(II), Ru(III), Os(II), Ir(I), Co(III), Co(II), Au(III), Au(I), *etc.*[7] Depending on the nature of metal, its oxidation state and the ligand, these complexes could elicit different cellular responses including redox imbalance, and target specific effects like DNA cross-linking/binding/intercalation, affecting the expression levels of functional proteins like p53, p21 and cyclin D1, inhibition of HIF-1a-p300 interaction, *etc.*[8–13]

Analogs of cisplatin, in general, are designed making use of simple diamines, peptide- or non-peptidic oligomers with built-in complexation sites, heterocyclic scaffolds and polymeric templates for Pt-coordination.[14–20] While chemotherapy with cisplatin analogs has significantly improved patient survival, new approaches which enable site-directed drug delivery, modulation of DNA interaction or type of cross-linking, and use of pro-drugs that release reactive Pt after cellular activation are currently being explored to improve and retain the effectiveness of this class of drugs.[21] Multinuclear Pt-complexes, characterized by the presence of more than one Pt center in one molecular framework, have gained attention as they could bring distinct types of DNA crosslinks compared to cisplatin.[22,23] A review by Wheate *et al.* has compared the activities of a large number of cisplatin analogs, in both mono- and multi-nuclear forms. In the case of the latter group, factors like spacing between reactive metal centers, their relative orientations, flexibility of the spacer, secondary interaction possibilities and charge are seen as the major contributory factors. These studies tend to show that a higher degree of flexibility in the spacer could increase the reactivity/extent of DNA cross-linking but at the expense of higher toxicity. Increased rigidity in the spacer, at the same time, leads to lower potency. In this context, a balanced flexibility could bring optimal reactivity with a better safety profile.[24] Since the conformation and flexibility of peptide segments can be controlled by varying the nature and sequence of building blocks, they offer an opportunity to study DNA cross-linking propensities and reactivities in a systematic manner.[25,26] They are also ideal for modulating tissue localization, cellular uptake

[a] *Department of Chemistry, Indian Institute of Technology Madras, Chennai, 600 036, India. E-mail: mkm@iitm.ac.in; Fax: +91-44 2257 4202; Tel: +91-44 2257 4233*

[b] *Department of Biotechnology, Indian Institute of Technology Madras, Chennai, 600 036, India. Fax: +91-44 2257 4102; Tel: +91-44 2257 4126*

† Electronic supplementary information (ESI) available. See DOI: 10.1039/c7nj03999a

‡ These authors contributed equally to this work.

and DNA interaction.[27] In this regard, synthetic protocols that allow introduction of platinum units at desired locations along the peptide sequences are important and are the theme of this report. In terms of mode of action, the peptide–Pt conjugates discussed in this manuscript are expected to be more close to cisplatin but the presence of peptide segments would allow fine-tuning of target interaction or cellular uptake.

Results and discussion

At first, we focused on identifying a bidentate ligand with a suitable anchoring point for peptide conjugation. Of different possibilities, diazides **3a–b** (Scheme 1), accessible from orthogonally protected serine and threonine through a reduction–mesylation–azidation sequence, seemed attractive as they can be attached to the peptide templates of interest through their carboxyl units. There have been reports on the use of 1,2,3-triaminopropane for preparing fluorescently labelled cisplatin analogs or similar conjugates with peptides, but these approaches involved the use of triaminopropane-1,3-dicarbamate, requiring acid-treatment followed by neutralization before platinum complexation.[28–32] In comparison, the diazides used in this report can be accessed and introduced into peptides rather easily and converted to the required diamines just before the complexation step. To obtain the simplest cisplatin analogs based on these ligands, azides **3a–b** were reduced under Pd/C and H_2 conditions and the diamines generated were reacted with K_2PtCl_4 in water to obtain complexes **4a–b** in 90–95% yields. The formation of **4a** was monitored by ^{1}H NMR experiments by noting shifts in CH and CH_2 signals after addition of K_2PtCl_4 (1 equiv.) in D_2O. There were considerable shifts in these peak positions, indicative of complexation, as shown in Fig. 1. The presence of platinum in the product was further confirmed by HRMS (ESI), which gave an isotope pattern for the mono-platinum complex with the molecular formula $C_8H_{19}Cl_2N_3O_2PtK$ corresponding to $[M + K]^+$ with m/z at 493.0149 (calcd 493.0139). It also showed a signal at −2970 ppm in ^{195}Pt NMR.

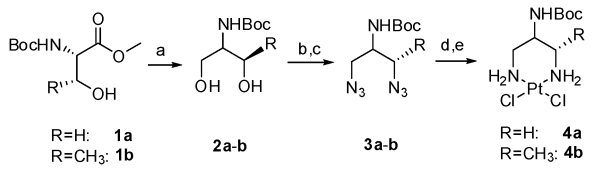

Scheme 1 *Reagents and conditions*: (a) $NaBH_4$/MeOH, 0 °C–rt, 24 h, 80–85%; (b) MsCl/Et_3N, CH_2Cl_2, 0 °C to rt; 2 h; (c) NaN_3, DMF, 60 °C, 12 h, 75–80%; (d) 10% Pd/C, H_2, MeOH, 2 h, 95–96%; and (e) K_2PtCl_4 (1 eq.), H_2O, 24 h, 90–95%.

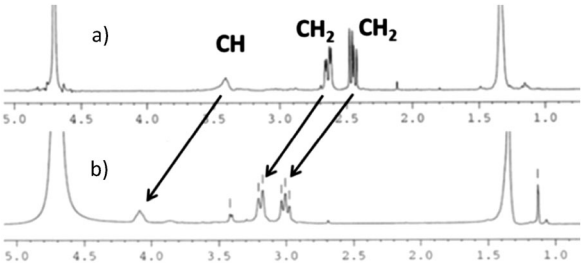

Fig. 1 ^{1}H NMR spectra of the 1,3-diamine derived from L-serine (a) and its platinum complex (b).

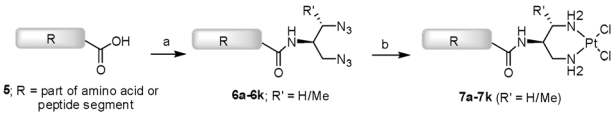

Scheme 2 *Reagents and conditions*: (a) free-amine from **3a** and **b**, EDC, HOBt, Et_3N, CH_2Cl_2, 0 °C to rt, 70–80%; and (b) (i) 10% Pd/C, H_2, MeOH; and (ii) K_2PtCl_4 (1 eq.), H_2O, 76–94%.

The feasibility of attaching the diamine equivalents **3a** and **b** to various amino acids and peptides is demonstrated in Scheme 2. Deprotection of the Boc group from **3a** and **b** and coupling of the free amine with appropriate Boc-protected amino acids or peptides (**5**) under EDC/HOBt conditions led to conjugates with the general structure **6a–k** in 70–80% yields. They were individually reduced and treated with K_2PtCl_4 in water to obtain the corresponding platinum complexes **7a–k** shown in Fig. 2.

Among them, the ornithine- and lysine based Pt conjugates **7d–7k** (Fig. 2) were prepared to make use of the electrostatic interaction of the side chain with the phosphate backbone of DNA to achieve additional stabilization to the Pt-complex. In fact, Reedijk *et al.* previously reported similar peptide–Pt conjugates from lysine and arginine, where the complexation was done through an ethylenediamine unit attached at the N-terminus.[33] The synthesis of **7h** starting from bis-Boc lysine (**8**) and ε-Boc LysOMe is shown in Scheme 3 as a representative example. The C-terminal deprotection and chain elongation of the initial adduct **9** can be done to introduce an appropriate number of lysine residues in the backbone and then capped with the diamine equivalent **3a** before taken for reduction and platination.

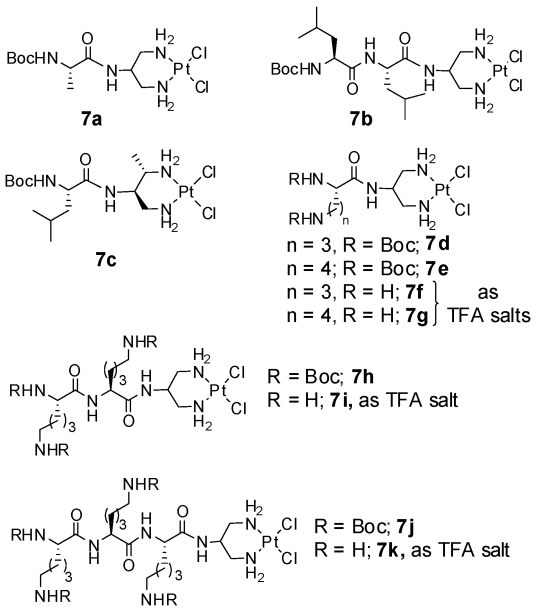

Fig. 2 Peptide platinum conjugates **7a–k**.

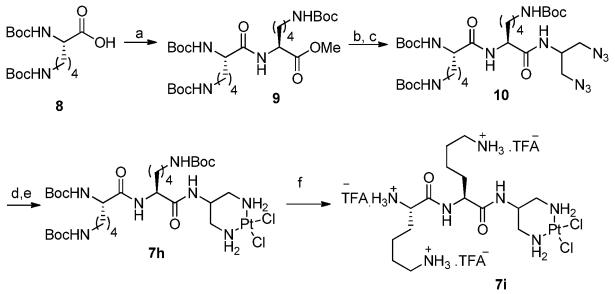

Scheme 3 *Reagents and conditions*: (a) H_2N-Lys(Boc)-OMe, EDC, HOBt, NEt_3, CH_2Cl_2, 68%; (b) LiOH, H_2O/THF (1 : 2), rt, 2 h, 94%; (c) free amine from **3a**, EDC, HOBt, NEt_3, CH_2Cl_2, 81%; (d) Pd/C, H_2, MeOH; (e) K_2PtCl_4, H_2O, 75%; and (f) CF_3CO_2H (neat), quantitative.

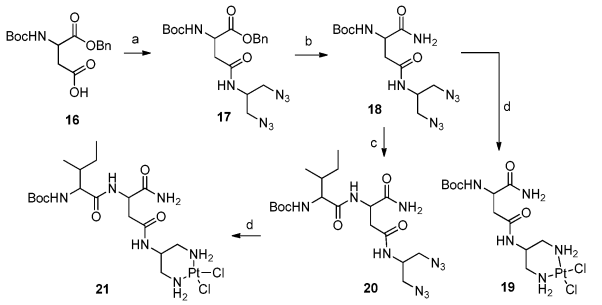

Scheme 5 *Reagents and conditions*: (a) free-amine from **3a**, EDC, HOBt, NEt_3, CH_2Cl_2, 0 °C to rt, 76%; (b) NH_3, methanol, rt, 6 h, 63%; (c) (i) TFA, CH_2Cl_2, rt; and (ii) Boc-Ileu-OH, EDC, HOBt, NEt_3, CH_2Cl_2, 0 °C to rt, 57%; and (d) (i) 10% Pd/C, H_2, MeOH; and (ii) K_2PtCl_4 (1 eq.), H_2O, 63%.

The next higher homologue **7j** was prepared following a similar sequence and the details are presented in the ESI.† The Boc-protected complexes **7d**, **7e**, **7h** and **7j** were individually treated with TFA to release the side chains as TFA salts which were also characterized by HRMS.

To introduce the ligand at any chosen location in the peptide sequence, we considered the aspartic acid side chain as a suitable anchoring point. Towards this, the key intermediate **12** (Scheme 4) was prepared by reacting N- and C-protected aspartic acid **11** with the free-amine from **3a**, and was subjected to azide reduction. Contrary to our expectation, diamine **13** underwent spontaneous cyclization to give imide **14**, which thwarted our progress through this route. For complete characterization, **14** was converted to its dinitrobenzamide derivative **15** and the spectral details are included in the ESI.†

Cyclization in peptides containing aspartic acid residues has previously been studied by Miklos Bodanszky and co-workers and is often a side reaction during the synthesis of aspartyl peptides.[34] We envisaged that amidation of the carboxyl terminus would decrease the cyclization propensity during the azide reduction step due to decreased electrophilicity. To know whether such an approach would work in the present context, BocAsp-(β-COOH)COOBn **16** (Scheme 5) was first prepared by RuO_4 oxidation of Boc-Phe-OBn[35] and coupled with the free-amine from **3a** under EDC/HOBt conditions to obtain **17** in 76% yield, and then treated with methanolic ammonia to obtain the C-terminal amide **18**. Subsequently, it was subjected to Boc-deprotection and coupled with Boc-Ileu-OH to obtain intermediate **20**, which upon reduction and platination gave the target compound **21** in 63% yield. It is also possible to reduce **18** and then prepare its platinum conjugate **19** in 67% without the problem of cyclization.

To prepare conjugate **26** (Scheme 6) having a platinum unit on the N-terminus residue, BocAsp(β-OMe)OH was first coupled with the free amine **23** (prepared from BocNHValPheOMe *via* amidation and Boc-deprotection). Here, the C-terminus is used in the form of carboxamide to discriminate it during the hydrolysis of N-terminal Asp-β-OMe. After treatment of **24** with LiOH, the resulting acid was coupled with the free-amine from **3a** and taken through reduction–platinum complexation steps to obtain product **26** in 80% yield.

Extension of this methodology to place multiple platinum centers on a peptide sequence is demonstrated in Scheme 7. Here, dipeptide **29** was first prepared from orthogonally protected coupling partners **27** and **28** in the solution phase. Methyl esters on N- and C-terminal residues were then hydrolysed using LiOH and the resulting diacid **30** was coupled with 2 equivalents of the free-amine from **3a** to obtain **31** in 69% yield. As done in the previous cases, reduction of **31** and platinum complexation afforded product **32a** as a brown coloured solid. The formation

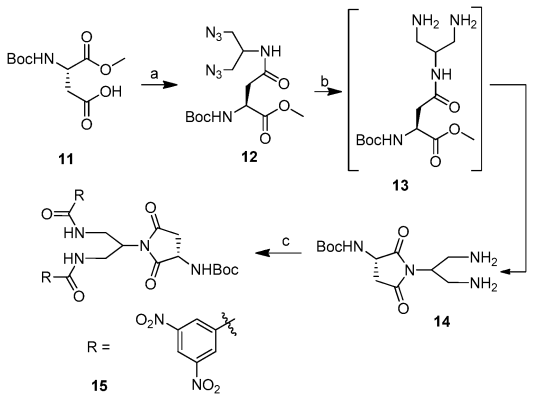

Scheme 4 *Reagents and conditions*: (a) free-amine from **3a** (1.2 eq.), EDC, HOBt, Et_3N, CH_2Cl_2, 0 °C to rt, 24 h, 70%; (b) 10% Pd/C, H_2, MeOH, 5 h, 95%; and (c) 3,5-dinitrobenzoyl chloride (2.2 eq.), Et_3N, CH_2Cl_2, 0 °C to rt, 5 h, 70%.

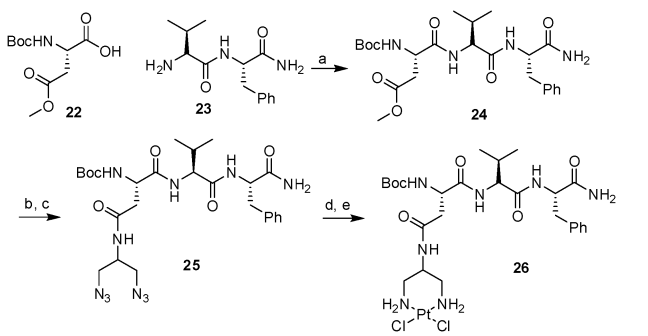

Scheme 6 *Reagents and conditions*: (a) EDC, HOBt, Et_3N, CH_2Cl_2, 0 °C to rt, 73%; (b) LiOH, THF/H_2O (2 : 1), rt, 85%; (c) free-amine from **3a** (1.2 eq.), EDC, HOBt, Et_3N, CH_2Cl_2, 0 °C to rt, 66%; (d) 10% Pd/C, H_2, MeOH, 94%; and (e) K_2PtCl_4 (1 eq.), H_2O, 78%.

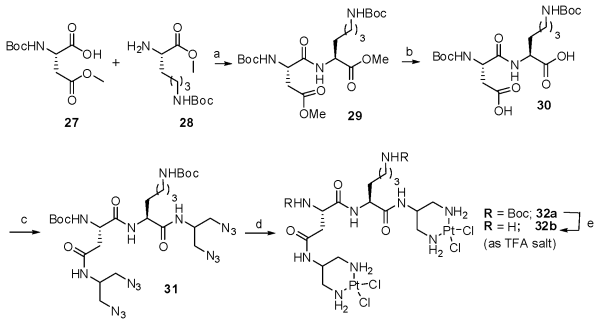

Scheme 7 *Reagents and conditions*: (a) EDC, HOBt, NEt_3, CH_2Cl_2, 12 h, 0 °C; (b) LiOH, H_2O/THF (1 : 2), 24 h; (c) free-amine from **3a**, EDC, HOBt, NEt_3, CH_2Cl_2, 0 °C to rt, 62%; (d) (i) Pd/C, H_2, MeOH, (ii) K_2PtCl_4, H_2O, 71%; and (e) TFA (neat).

of this complex was confirmed by HRMS (ESI), which gave a peak at m/z = 1098.6023 corresponding to the molecular formula $C_{26}H_{53}Cl_3N_9O_7Pt_2$ $[M - Cl]^+$ with two platinum atoms. The isotope pattern in agreement with the theoretical values is included in the ESI.†

DNA interaction studies: ethidium bromide displacement assay

Ethidium bromide (EtBr) displacement assay is commonly followed to assess the DNA binding affinity of various intercalators and binders from natural and synthetic sources.[36–38] This cationic dye exhibits strong emission at around 600 nm (when excited at 526 nm) on intercalation between the base pairs of DNA, but displacement with other molecules leads to decrease in emission intensity.[39–41] At first, a stock solution of calf thymus DNA was prepared in Tris–HCl buffer (50 mM Tris, 10 mM NaCl, pH 7.4). The ratio of absorbance of this solution at 260 and 280 nm (A_{260}/A_{280}) was found to be in the 1.8–1.9 range, indicating that the influence from proteins is minimal.[42] The concentration of this stock solution was determined on the basis of UV absorbance at 260 nm and the reported molar extinction coefficient of 6600 M^{-1} cm^{-1} for CT DNA, and was estimated to be 3.32×10^{-4} M.[43] For fluorescence studies, the peptide–Pt conjugates were dissolved in 10% DMSO in Tris–HCl buffer (50 mM Tris, 10 mM NaCl, pH 7.4), whereas an ethidium bromide solution was prepared in Millipore water. Fluorescence measurements were performed using a Jasco spectrofluorometer at an excitation wavelength of 526 nm and emission was observed at 605 nm. Emission spectra were recorded with increasing amounts of the Pt complex by adding 10 μL of 10 mM solution each time. In these experiments, the intensity of the emission at 605 nm was found to decrease with increase in the concentration of peptide–Pt conjugates. The emission profiles of **4a**, **7e**, **32a** and **7i** are presented in Fig. 3 and those of others are included in the ESI† (Fig. S88). The peptide–Pt conjugates **4a–b**, **7a–e**, **7h**, **7j** and **7f**, **7g**, **7i**, **7k** allow us to understand the effect of positive charge on the side chain to their DNA interaction. The former group, having the side chain in the Boc-protected form, was relatively less efficient compared to the latter, which have free amino groups as triflate salts.

As evident from Fig. 4(e) the slopes of the Stern–Volmer plots in the case of systems with positively charged side chains

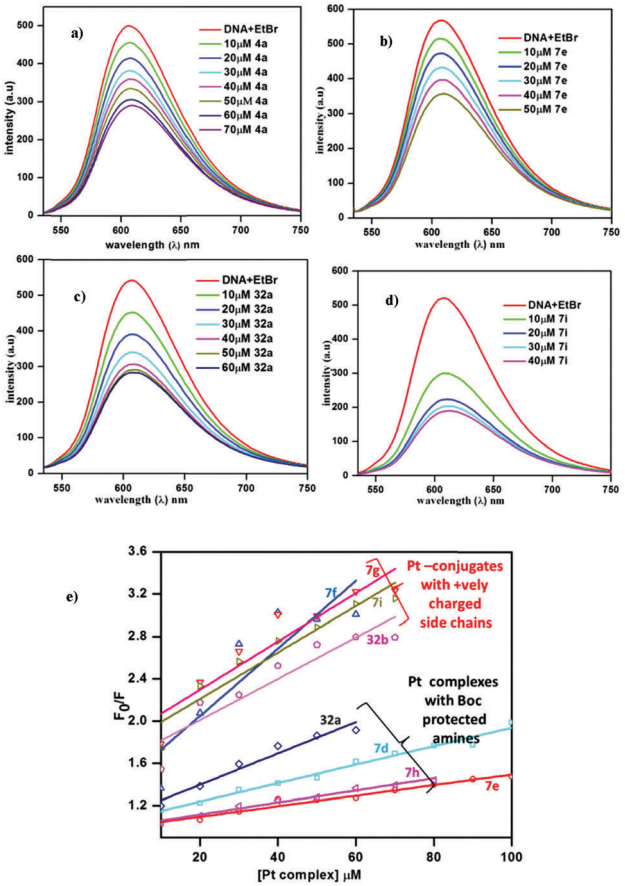

Fig. 3 Variation in fluorescence intensity from ethidium bromide upon increasing the concentration of **4a** (a), **7e** (b), **32a**, (c) and **7i** (d); [DNA] = 1.5×10^{-5} M, [EtBr] = 1.5×10^{-5} M. Comparison of Stern–Volmer plots obtained from various experiments showing relatively better binding profiles of positively charged Pt conjugates as indicated by their slopes (e).

(**7f**, **7g**, **7i** and **32b**) are greater than those of the analogous uncharged ones (**7d**, **7e**, **7h** and **32a**), which supports the fact that an increase in the number of charges has a positive influence on DNA interaction which is expected based on the electrostatic interaction with the phosphate backbone. Apparent binding constants are useful for comparing compounds which interact with DNA. A K_{app} value above 10^6 M^{-1} indicates the classical intercalation like EtBr, whereas the value in the 10^4–10^5 M^{-1} range represents the groove binding. Although cisplatin analogs interact with DNA through a different mechanism, their relative affinities with DNA have been correlated using K_{app}.[44] To make some comparative assessment, the apparent binding constants (K_{app}) of the complexes were calculated using the equation

$$K_{EB}[EB] = K_{app}[complex]$$

where K_{EB} is the DNA binding constant of EtBr (1.0×10^7 M^{-1}), [EB] is the concentration of ethidium bromide and [complex] is the concentration of the Pt complex at 50% reduction of the initial fluorescence emission intensity of EB bound DNA. The K_{app} values for various complexes are given in Table 1. It is very interesting to note that at least two compounds (**7i** and **7k**) from

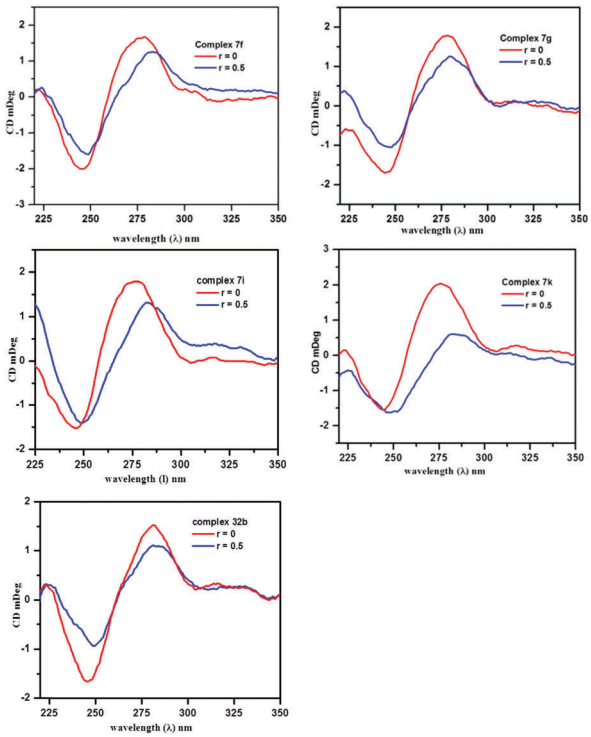

Fig. 4 Results obtained from CD analysis indicative of changes in the DNA conformation in the presence of Pt-complexes **7f**, **7g**, **7i**, **7k** and **32b**; r = [complex]/[DNA]; r = 0 represents only DNA.

Table 1 Apparent binding constants (K_{app}) of peptide–platinum conjugates

Pt conjugate	K_{app} ($\times 10^5$ M^{-1})	Pt conjugate	K_{app} ($\times 10^5$ M^{-1})
4a	0.82	**7g**	30.45
4b	1.12	**7h**	2.99
7a	2.09	**7i**	106.70
7b	1.52	**7j**	5.90
7c	2.03	**7k**	115.20
7d	2.19	**26**	8.01
7e	2.51	**32a**	3.99
7f	32.03	**32b**	62.80

this series have K_{app} values in the order of 10^7 that are comparable with EtBr.

CD spectroscopic studies

Circular dichroism is a sensitive technique to study the conformational changes of DNA during interaction with a drug or binding agent. Normally, the CD spectrum of calf thymus DNA shows a positive CD signal at 275 nm, and a negative CD signal at 245 nm. This is attributed to base-stacking and right handed helicity, respectively. Disturbance in the helicity of base stacking in the presence of a chemical compound can be monitored from the changes in its CD spectrum. CD measurements for Pt-complexes **7f**, **7g**, **7i**, **7k** and **32b**, which are soluble in water, were performed using a Chirascan CD spectrometer. A 10 mm quartz cuvette was used for the study. Platinum complexes and DNA were dissolved in Tris–HCl buffer (50 mM Tris, 10 mM NaCl, pH 7.4). Significant changes in the CD spectrum upon addition of these compounds to DNA solution (r = 0, 0.5, where r = [complex]/[DNA]) confirm that these complexes interact well with DNA and induce changes in its conformation (Fig. 4).

Anticancer assay

Based on the promising results from the ethidium bromide displacement assay, the cytotoxicities of these platinum conjugates were evaluated on human cervical cancer cells (SiHa) following Alamar blue assay.[45,46] The dose–response plots of selected compounds are shown in Fig. 5 and those of others are included in the ESI† (Table S1). As can be seen, there was a dose-dependent decrease in cell-viability with increase in the concentration of these conjugates. In general, the presence of positively charged side chains led to a better cytotoxic response compared to those containing hydrophobic groups (**7i**, **7k** *vs.* **7a**, **7b**). The bis-platinum complex in the Boc-protected form (**32a**) and as salt (**32b**) showed comparable activities (IC_{50} values 75.9 μM and 83.4 μM), which could be due to the formation of distinct types of DNA cross-links with less influence from the side chains. The advantage of having multiple positive charges becomes evident if we compare the activity of **7i** with three positive charges (IC_{50} 44.5 μM, Table 1) with that of **7g** (IC_{50} 98.1 μM), which is the lower homologue; increase in cellular uptake and better phosphate binding could be responsible. In fact, this is in agreement with the observations from the ethidium bromide displacement assay where an increase in the number of lysine residues was found to positively influence DNA interaction. In comparison with cisplatin (IC_{50} 25.3 μM), **7i** and **7k** showed IC_{50} values of 44.5 μM and 51.1 μM upon incubation for 48 h (Table 2, entries 6 and 7). To rule out the possibility of ligands alone contributing to the cytotoxic effect, the free amines of **4a**, **7d**, **7e**, **32a**, **7f**, **7g**, and **32b** were also tested for their anti-cancer activities against SiHa cell lines at 24 h, 48 h and 72 h using the Alamar blue assay. Their IC_{50} values were >200 μM, and distinctly different from those of the corresponding Pt conjugates (Fig. S86, ESI†). We also tested these compounds against normal mouse fibroblastic cell lines (NiH3t3) for assessing safety. Their therapeutic index (TI) values were either comparable to or better than that of cisplatin (Fig. S87 and Table S2, ESI†). Although the relative activity is

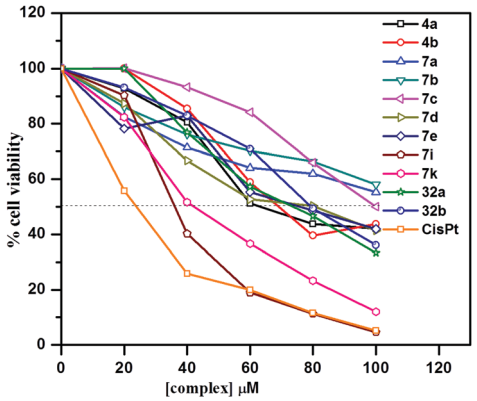

Fig. 5 Dose–response plots of the peptide–Pt conjugates in the assay against SiHa cells after incubation for 48 h.

Table 2 IC_{50} values of the peptide–platinum conjugates (after incubation for 48 h)

Sl no.	Pt conjugate	IC_{50} (μM) ± std dev.	Sl no.	Pt conjugate	IC_{50} (μM) ± std dev.
1	**4a**	77.7 ± 0.0041	6	**7i**	44.5 ± 0.0101
2	**4b**	80.5 ± 0.0038	7	**7k**	51.1 ± 0.0028
3	**7a**	99.7 ± 0.0085	8	**32a**	75.9 ± 0.0046
4	**7b**	116.5 ± 0.0017	9	**32b**	83.4 ± 0.0062
5	**7g**	98.1 ± 0.0144	10	Cisplatin	25.3 ± 0.0041

lower, the methodology developed here offers an opportunity to fine-tune the backbone composition and position of the Pt centers, which should allow us to identify better leads. The cytotoxicities of these compounds and related derivatives against different types of cancer cell lines will be investigated in detail and a complete structure–activity relationship study will be communicated in due course.

Conclusions

Knowing the importance of cisplatin in cancer chemotherapy and the need to develop new analogs to overcome resistance, the objective of the present study was to use diamines generated from serine and threonine as ligands for platinum complexation in a peptide environment. Towards this, the side-chain and α-carboxyl groups of Ser and Thr were modified to azidomethylene units and then connected to various peptides through the central amino group. The resulting diazide derivatives of peptides were subjected to reduction and platinum complexation to obtain the target compounds in good yields. This included peptide–Pt conjugates with the metal at the C-terminus and N-terminus and on both ends. These compounds induced dose-dependent changes in DNA, which was studied by ethidium bromide displacement assay. The presence of multiple positive charges on the peptide side chains was found to favor DNA interaction, which was also reflected in their cytotoxic response. The methodology presented here allows the synthesis of new analogs with better cytotoxic and selectivity profiles for development.

Experimental

General methods and materials

All amino acids and reagents were purchased from SRL Pvt. Ltd or Spectrochem Pvt. Ltd and used as received. Potassium tetrachloroplatinate, calf thymus DNA and ethidium bromide were purchased from Sigma Aldrich. Solvents were dried following standard procedures. ^{1}H NMR and ^{13}C NMR spectra were recorded on Bruker Avance 400 MHz and 500 MHz instruments. The chemical shifts are reported in parts per million (ppm) relative to tetramethylsilane, with *J* values in Hertz. ^{13}C NMR spectral data are reported with the solvent peak ($CDCl_3$ at 77.16 ppm and DMSO-d_6 at 39.52 ppm) as the internal standard. ^{195}Pt NMR was recorded on a 500 MHz instrument and chemical shifts were reported relative to K_2PtCl_4 (δ = −1617 ppm) as an external standard. High-resolution mass spectra (HRMS) were recorded on a Waters Q-Tof *micro*™ spectrometer with a LockSpray source. Infrared spectra were recorded using a Nicolet 6700 FT-IR spectrophotometer. Fluorescence measurements were performed using a Jasco spectrofluorometer and circular dichroism measurements were performed using a Chirascan CD spectrometer.

Synthesis of diazides 3a and 3b. Methyl esters of L-serine and L-threonine were first prepared in quantitative yields by stirring their MeOH solutions with $SOCl_2$ (2 eq.) under ice-cold conditions. *N*-Boc protection of these esters was done by treatment with Boc-anhydride (1.1 eq.) in the presence of triethylamine (2 eq.) in dichloromethane to obtain **1a** and **1b** in 95% yields. These Boc-protected esters were reduced to the corresponding alcohols **2a** and **2b** (85–95%) using $NaBH_4$ (2 eq.) in methanol (*Chem. Pharm. Bull.*, 1985, **33**, 1342). Mesylation of **2a** and **2b** using mesyl chloride, followed by azide substitution with sodium azide (2.5 eq.), gave diazides **3a** and **3b** in 80–95% yields.

General procedure for the preparation of peptide–platinum complexes. To a stirred solution of the diamine (1 eq.) in HPLC grade water (1 mL/10 mg), K_2PtCl_4 (1 eq.) was added, and the mixture was allowed to stir for 24–48 h under dark conditions. Once the starting materials were consumed, a yellow or light brown precipitate formed was filtered under vacuum under protection from light, and washed with water and diethyl ether to obtain the platinum complex in 55–95% yields.

Cell culture. Cells (SiHa and NiH3t3) were maintained as adherent monolayers in a tissue culture flask fed with complete DMEM (Gibco) supplemented with 10% (v/v) fetal bovine serum (FBS) containing 100 mg L^{-1} penicillin and 66.6 mg L^{-1} streptomycin. The cells were incubated in a humidified incubator at 37 °C with 5% CO_2. During the experiment the cells were washed using 1× PBS–EDTA, trypsinized using 0.25% trypsin, neutralized with complete DMEM, and centrifuged at 2000 rpm for 5 min, and the supernatant was aspirated, whereas the pellet was suspended in complete DMEM for seeding or culturing.

Cytotoxicity assay. The cell viability was assessed using the Alamar blue reagent, resazurin (7-hydroxy-10-oxidophenoxazin-10-ium-3-one). Briefly, 4000 cells per well were seeded into 96 well plates and allowed to adhere overnight. The cells were treated with different concentrations of cisplatin and analogs for 24 h, 48 h and 72 h. At the end of each time point, 10 μL of Alamar blue (1 mg mL^{-1}) was added and mixed well. The plate was incubated at 37 °C with 5% CO_2 for 3 h. The colour developed was read as optical density (OD) using a Bio-Rad 680 model colorimeter at 570 nm with 595 nm as a background reference.

Diazide 3a. Colorless liquid; yield = 80%; R_f (EtOAc/hexane, 1 : 3), 0.3; ^{1}H NMR ($CDCl_3$, 500 MHz): δ 4.83 (bs, 1H), 3.87 (bs, 1H), 3.53–3.50 (dd, 2H, *J* = 12.38, 4.57 Hz), 3.43–3.39 (dd, 2H, *J* = 12.38, 5.91 Hz), 1.43 (s, 9H) ppm; ^{13}C NMR ($CDCl_3$, 125 MHz): δ 155.0, 80.4, 51.8 (2C), 49.4, 28.4 (3C) ppm; IR (KBr): 2923, 2896, 2102, 1703, 1683, 1354, 1195 cm^{-1}; HRMS (ESI) exact mass calcd for $C_8H_{15}N_7O_2Na$ $[M + Na]^+$ 264.1185, found 264.1199.

Pt-Conjugate 4a. Orange solid; yield = 95%; ^{1}H NMR (DMSO-d_6, 400 MHz): δ 7.19–6.97 (m, 1H), 5.85–5.68 (bs, 2H), 5.60–5.43 (bs, 1H),

5.40–4.94 (m, 1H), 3.83–3.60 (bs, 1H), 2.76–2.66 (m, 1H), 2.65–2.53 (m, 2H), 2.48–2.34 (m, 1H), 1.38 (s, 9H) ppm; ^{195}Pt NMR (DMSO-d_6, 107 MHz): δ = −2970 ppm; HRMS (ESI) exact mass calcd for $C_8H_{19}Cl_2N_3O_2PtK$ $[M + K]^+$ 493.0139, found 493.0149, isotopic peaks *m*/*z* 492, 493, 494, 495, 496.

Diazide 3b. Colourless liquid; yield = 80%; R_f (EtOAc/hexane, 1 : 3), 0.3; ^{1}H NMR ($CDCl_3$, 500 MHz): δ 4.80 (d, 1H, J = 7.4 Hz), 3.71–3.56 (m, 3H), 3.46–3.43 (dd, 1H, J = 12.5, 3.7 Hz), 1.45 (s, 9H), 1.34 (d, 3H, J = 6.5 Hz) ppm; ^{13}C NMR ($CDCl_3$, 125 MHz): δ 155.3, 80.4, 58.3, 53.8, 51.5, 28.4 (3C), 16.2 ppm; IR (KBr): 2936, 2889, 2102, 1700, 1526, 1519 cm^{-1}; HRMS (ESI) exact mass calcd for $C_9H_{17}N_7O_2Na$ $[M + Na]^+$ 256.1522, found 256.1493.

Pt-Conjugate 4b. Brown solid; yield = 90%; HRMS (ESI) exact mass calcd for $C_9H_{21}Cl_2N_3O_2PtNa$ $[M + Na]^+$ 491.0556, found 491.0570; isotopic peaks: 489, 490, 491, 492, 493; ^{195}Pt NMR (107 MHz, DMSO-d_6): δ = −2992 ppm.

Diazide 6a (precursor of 7a). White solid; yield = 94%; ^{1}H NMR ($CDCl_3$, 400 MHz): δ 6.96 (bs, 1H), 5.30 (bs, 1H), 4.18 (bs, 2H), 3.57–3.40 (m, 4H), 1.46 (s, 9H), 1.36 (d, 3H, J = 4.6 Hz) ppm; ^{13}C NMR ($CDCl_3$, 100 MHz): δ 173, 156, 80.6, 51.5, 51.4, 50.2, 48.1, 28.4 (3C), 17.7 ppm; IR (KBr): 2929, 2879, 2099, 1715, 1679, 1348 cm^{-1}; HRMS (ESI) exact mass calcd for $C_{11}H_{21}N_8O_3$ $[M + H]^+$ 313.1731, found 313.1719.

Pt-Conjugate 7a. Yellow solid; yield = 94%; ^{195}Pt NMR (107 MHz, DMSO-d_6): δ = −2992 ppm; HRMS (ESI) exact mass calcd for $C_{11}H_{24}Cl_2N_4O_3PtK$ $[M + K]^+$ 564.0510, found 564.0524, *m*/*z* 563, 564, 565, 566, 567.

Diazide 6b (precursor of 7b). White solid; yield = 85%; R_f (EtOAc/hexane, 1 : 3), 0.2; ^{1}H NMR ($CDCl_3$, 400 MHz): δ 7.15–7.00 (bs, 1H), 6.77–6.11 (bs, 1H), 5.14–4.97 (bs, 1H), 4.50–4.38 (m, 1H), 4.18–4.01 (m, 2H), 3.57–3.34 (m, 4H), 1.75–1.48 (m, 6H), 1.44 (s, 9H), 0.96–0.85 (m, 12H); ^{13}C NMR ($CDCl_3$, 100 MHz): δ 172.8, 171.9, 155.7, 80.6, 51.9, 51.2, 48.4, 40.6, 40.4, 28.3 (3C), 24.8 (2C), 24.7 (2C), 23.0, 22.9, 21.8 (2C) ppm; IR (KBr): 3096, 2927, 2102, 1711, 1671, 1630, 1542, 1345, 1297, 1254, 1202, 1163, 1078, 918, 728, 664 cm^{-1}; HRMS (ESI) exact mass calcd for $C_{20}H_{37}N_9O_4Na$ $[M + Na]^+$ 490.2866, found 490.2872.

Pt-Conjugate 7b. Yellow solid; yield = 84%; ^{195}Pt NMR (107 MHz, DMSO-d_6): δ = −2962 ppm; HRMS (ESI) exact mass calcd for $C_{20}H_{41}Cl_2N_5O_4PtNa$ $[M + Na]^+$ 703.2081, found 703.2065, *m*/*z* 702, 703, 704, 705, 706.

Diazide 6c (precursor of 7c). White solid; yield = 82%; R_f (EtOAc/hexane, 1 : 3), 0.2; ^{1}H NMR ($CDCl_3$, 500 MHz): δ 6.61 (bs, 1H), 4.94 (bs, 1H), 4.06–3.99 (m, 2H), 3.66–3.61 (m, 2H), 3.46–3.43 (m, 1H), 1.91–1.86 (m, 1H), 1.67–1.66 (m, 2H), 1.44 (s, 9H), 1.31 (d, 3H, J = 6.4 Hz), 0.94 (t, 6H, J = 6.2 Hz) ppm; ^{13}C NMR ($CDCl_3$, 125 MHz): δ 172.7, 156.0, 80.5, 57.8, 53.4, 52.3, 51.4, 40.5, 28.4 (3C), 24.9, 22.9, 22.2, 16.1 ppm; IR (KBr): 2961, 2929, 2102, 1682, 1366, 1286, 1055, cm^{-1}; HRMS (ESI) exact mass calcd for $C_{15}H_{28}N_8O_3Na$ $[M + Na]^+$ 391.4346, found 391.4326.

Pt-Conjugate 7c. Orange-yellow solid; yield = 95%; ^{195}Pt NMR (107 MHz, DMSO-d_6): δ = −2967 ppm; HRMS (ESI) exact mass calcd for $C_{15}H_{32}Cl_2N_4O_3PtK$ $[M + K]^+$ 620.1136, found 620.1150, *m*/*z* 619, 620, 621, 622, 623.

Diazide 6d (precursor of 7d). White solid; yield = 63%; R_f (EtOAc/hexane, 1 : 3), 0.2; ^{1}H NMR (400 MHz, $CDCl_3$): δ 6.94–6.75 (bs, 1H), 5.25–5.11 (bs, 1H), 4.78–4.65 (m, 1H), 4.27–4.11 (m, 2H), 3.58–3.39 (m, 4H), 3.35–3.31 (m, 1H), 3.13–3.01 (m, 1H), 1.87–1.84 (bs, 1H), 1.63–1.50 (m, 3H), 1.43 (s, 18H) ppm; ^{13}C NMR (100 MHz, $CDCl_3$): δ 172.5, 156.7, 156.0, 80.4, 79.6, 53.6, 51.5, 51.4, 48.3, 39.6, 29.8, 28.5 (3C), 28.4 (3C), 26.5 ppm; IR (neat): 2926, 2102, 1654, 1169 cm^{-1}; HRMS (ESI) exact mass calculated for $C_{18}H_{33}N_9O_5Na$ $[M + Na]^+$ 478.2502, found 478.2522.

Pt-Conjugate 7d. Brown solid, yield = 70%, ESI-MS *m*/*z*, 711 $[M - Cl + DMSO]^+$; isotopic pattern *m*/*z*: 710, 711, 712, 713, 714; ^{195}Pt NMR (107 MHz) δ −2953.9 ppm.

Pt-Conjugate 7f. Brown-coloured hygroscopic solid; yield = quantitative; ESI-MS: *m*/*z* 470 corresponding to $C_8H_{22}Cl_2N_5OPt$ $[M + H]^+$, isotopic mass 468, 469, 470, 471, 472; *m*/*z* 434 ($C_8H_{21}ClN_5OPt$ $[M - Cl]^+$), isotopic mass 432, 433, 434, 435, 436.

Diazide 6e (precursor of 7e). Colorless liquid; yield = 69%; R_f (EtOAc/hexane, 1 : 3), 0.2; ^{1}H NMR (500 MHz, $CDCl_3$): δ 6.85–6.56 (bs, 1H), 5.40–5.23 (bs, 1H), 4.66 (bs, 1H), 4.18–4.16 (m, 1H), 4.02 (bs, 1H), 3.58–3.40 (m, 4H), 3.17–3.03 (bd, 2H), 1.89–1.81 (bs, 2H), 1.68–1.55 (bs, 2H), 1.46–1.40 (m, 20H) ppm; ^{13}C NMR (125 MHz, $CDCl_3$): δ 172.5, 156.5, 156.1, 80.5, 79.4, 54.7, 51.5, 51.4, 48.1, 39.7, 31.4, 29.8, 28.6 (3C), 28.4 (3C), 22.6 ppm; IR (neat): 3316, 2925, 2856, 2102, 1690, 1523, 1169 cm^{-1}; HRMS (ESI) exact mass calculated for $C_{19}H_{35}N_9O_5Na$ $[M + Na]^+$ 492.2659, found 492.2672.

Pt-Conjugate 7e. Brown solid; yield = 76%, ^{195}Pt NMR (107 MHz) δ −2953.9 ppm; HRMS (ESI): exact mass calculated for $C_{19}H_{39}Cl_2N_5O_5PtNa$ $[M + Na]^+$ 705.1874, found 705.1854; ESI-MS: *m*/*z* 679 $[M - Cl + CH_3OH]^+$, isotopic peaks 677, 678, 679, 680, 681.

Pt-Conjugate 7g. Brown color hygroscopic solid; yield = quantitative; HRMS (ESI) exact mass calculated for $C_9H_{24}N_5OCl_2Pt$ $[M + H]^+$ 483.1006, found 483.0995, isotopic peaks *m*/*z* 482, 483, 484, 485, 486, 487, 488.

Diazide 6h (precursor of 7h). White solid; yield = 61%; R_f (EtOAc/hexane, 1 : 1), 0.3; ^{1}H NMR (400 MHz, $CDCl_3$): δ 7.06 (bs, 1H), 6.67 (bs, 1H), 5.56 (bs, 1H), 4.88–4.63 (m, 2H), 4.38–4.30 (m, 1H), 4.19–4.10 (m, 1H), 4.05–3.95 (bs, 1H), 3.57–3.39 (m, 4H), 3.15–3.04 (m, 4H), 1.83–1.79 (bs, 5H), 1.69–1.66 (m, 2H), 1.50–1.39 (m, 32H) ppm; ^{13}C NMR (100 MHz, $CDCl_3$): δ 172.7, 171.8, 156.8, 156.3, 80.8, 79.5, 55.5, 53.5, 51.5, 51.4, 48.8, 40.13, 39.3, 31.2, 30.0, 29.8, 29.6, 28.6 (3C), 28.5 (3C), 28.4 (3C), 22.9, 22.3 ppm; IR (neat): 3304, 2976, 2931, 2102, 1693, 1170 cm^{-1}; HRMS (ESI) exact mass calculated for $C_{30}H_{55}N_{11}O_8Na$ $[M + Na]^+$ 720.4133, found 720.4122.

Pt-Conjugate 7h. Dark brown solid; yield = 55%; ^{195}Pt NMR (107 MHz): δ −2953.435 ppm; HRMS (ESI): exact mass calculated for $C_{30}H_{59}N_7O_8Cl_2PtNa$ $[M + Na]^+$ 933.3348, found 933.3351, isotopic peaks 932, 933, 934, 935, 936, 937.

Pt-Conjugate 7i. Brown color hygroscopic solid; yield = quantitative; HRMS (ESI) exact mass calculated for $C_{15}H_{36}N_7O_2Cl_2Pt$ $[M + H]^+$ 611.1955, found 611.1977, isotopic peaks 610, 611, 612, 613, 614, 615, 616.

Diazide 6j (precursor of 7j). Gummy liquid; yield = 55%; R_f (EtOAc/hexane, 7 : 3), 0.4; ^{1}H NMR (400 MHz, $CDCl_3$): δ 7.17–7.06 (bs, 1H), 6.86–6.65 (bs, 1H), 5.67–5.31 (bs, 1H), 5.04–4.65 (m, 3H), 4.48–3.84 (m, 4H), 3.59–3.34 (m, 4H), 3.23–2.96 (m, 6H), 1.94–1.36 (m, 54H) ppm; IR (neat): 3219, 2988, 2936, 2102, 1677, 1207 cm^{-1}; HRMS (ESI) exact mass calculated for $C_{41}H_{75}N_{13}O_{11}Na$ $[M + Na]^+$ 948.5607, found 948.5637.

Pt-Conjugate 7j. Brown color solid; ESI-MS: *m*/*z* 1177 ($C_{41}H_{79}Cl_2N_9O_{11}PtK$ $[M + K]^+$), isotopic peaks 1176, 1177, 1178, 1179, 1180, 1181.

Pt-Conjugate 7k. Brown color hygroscopic solid; yield = quantitative; HRMS (ESI) exact mass calculated for $C_{21}H_{48}N_9O_3Cl_2Pt$ $[M + H]^+$, 739.2905, found 739.2933, isotopic peaks 738, 739, 740, 741, 742, 743, 744.

Diazide 12. White solid; yield = 70%; R_f (EtOAc/hexane, 1 : 3), 0.5; ^{1}H NMR ($CDCl_3$, 500 MHz): δ 6.89 (bs, 1H), 5.70 (d, 1H, *J* = 6.8 Hz), 4.45 (bs, 1H), 4.13–4.12 (m, 1H), 3.68 (s, 3H), 3.53–3.49 (m, 2H), 3.43–3.40 (m, 2H), 2.97–2.91 (m, 1H), 2.67 (dd, 1H, *J* = 17.0, 5.9 Hz), 1.43 (s, 9H) ppm; ^{13}C NMR ($CDCl_3$, 125 MHz): δ 172.4, 171.0, 155.8, 80.9, 52.2 (2C), 51.3, 50.7, 48.2, 35.6, 28.3 (3C) ppm; IR (KBr, neat): 2970, 2933, 2102, 1641, 1528, 1447, 1367, 1269, 968, 743, 699, 672 cm^{-1}; HRMS (ESI) exact mass calcd for $C_{13}H_{22}N_8O_5Na$ $[M + Na]^+$ 393. 1611, found 393.1624.

Compound 15. White solid; yield = 70%; R_f (EtOAc/hexane, 1 : 3), 0.2; $[\alpha]_D^{25}$ −14.05 (c 1, $CHCl_3$); ^{1}H NMR (DMSO-d_6, 500 MHz): δ 9.35 (t, *J* = 5.5 Hz, 1H), 9.30–9.26 (m, 1H), 9.01 (bs, 2H), 8.98–8.97 (m, 2H), 8.96–8.94 (m, 2H), 7.42 (d, *J* = 7.9 Hz, 1H), 4.57–4.50 (m, 1H), 4.24–4.20 (q, *J* = 7.6 Hz, 1H), 3.93–3.88 (m, 1H), 3.81–3.79 (t, *J* = 12.25 Hz, 2H), 3.68–3.59 (m, 1H), 2.93 (dd, *J* = 17.45, 9.25 Hz, 1H), 2.56 (dd, *J* = 17.50, 5.90 Hz, 1H), 1.20 (s, 9H) ppm; ^{13}C NMR (125 MHz, DMSO-d_6): δ 176.7, 175.1, 162.5 (2C), 162.3 (2C), 154.9, 148.19 (2C), 148.15 (2C), 136.8(2), 136.7(2), 127.4, 127.3, 120.9, 120.8, 78.7, 50.9, 48.9, 34.9, 27.7 (3C) ppm; IR (KBr): 3096, 2927, 1711, 1671, 1630, 1542, 1345, 1297, 1254, 1202, 1163, 1078, 918, 728, 664 cm^{-1}; HRMS (ESI) exact mass calcd for $C_{26}H_{26}N_8O_{14}Na$ $[M + Na]^+$ 697.1466, found 697.1467.

Diazide 18 (precursor of 19). White solid; yield = 55%; R_f (EtOAc/hexane, 9 : 1), 0.2; ^{1}H NMR ($CDCl_3$, 400 MHz): δ 7.46 and 7.00 (bs, 1H), 6.91 and 6.34 (bs, 1H), 6.28–5.93 (m, 2H), 4.63–4.36 (bs, 1H), 4.23–4.02 (bs, 1H), 3.60–3.35 (m, 4H), 2.93–2.78 (m, 1H), 2.65–2.55 (dd, 1H), 1.44 (s, 9H) ppm; ^{13}C NMR ($CDCl_3$, 100 MHz): δ 174.2, 171.1, 155.8, 80.6, 51.3 (2C), 48.2, 37.6, 36.9, 28.3 (3C) ppm; IR (neat): 3304, 2976, 2931, 2102, 1693, 1170 cm^{-1}; HRMS (ESI) exact mass calcd for $C_{12}H_{22}N_5O_4$ $[M + H]^+$ 356.1795, found 356.1811.

Pt-Conjugate 19. Orange coloured solid; yield = 49%; HRMS (ESI) calculated for $C_{12}H_{25}N_5O_4Cl_2PtK$ $[M + K]^+$, 607.0569, found 607.0582, isotopic peaks 605, 606, 607, 608, 609; *m*/*z* 533, $[M - Cl]^+$, isotopic peaks 532, 533, 534, 535, 536.

Diazide 20 (precursor of 21). White solid; yield = 56%; R_f (EtOAc/hexane, 3 : 1), 0.2; ^{1}H NMR ($CDCl_3$, 500 MHz): δ 8.10–7.93 (bs, 2H), 7.33–7.06 (bs, 1H), 6.41–6.16 (bs, 1H), 6.16–5.87 (m, 1H), 4.83–4.67 (m, 1H), 4.16–4.06 (bs, 1H), 4.01–3.83 (m, 1H), 3.56–3.35 (m, 4H), 2.89–2.74 (m, 1H), 2.68–2.57 (m, 1H), 1.91–1.77 (bs, 1H), 1.45 (s, 9H), 1.31–1.16 (m, 2H), 0.97–0.86 (m, 6H) ppm; ^{13}C NMR ($CDCl_3$, 125 MHz): δ 172.5, 171.5, 168.6, 153.8, 80.1, 60.8, 52.0 (2C), 50.5, 49.1, 37.7, 29.1 (3C), 25.6, 16.4, 12.3, 11.9 ppm; IR (KBr): 2984, 2986, 2105, 1749, 1717, 1672, 1445, 1422, 1048, 895, 667, 580 cm^{-1}; HRMS (ESI) exact mass calcd for $C_{18}H_{33}N_{10}O_5$ $[M + H]^+$ 469.2635, found 469.2646.

Pt-Conjugate 21. Orange colour solid; yield = 62%; ESI-MS, *m*/*z* 646 $[M - Cl]^+$ with mol. formula $[C_{18}H_{36}ClN_6O_5Pt]^+$, isotopic peaks 645, 646, 647, 648, 649.

Diazide 25 (precursor of 26). White solid; yield = 62%; R_f (EtOAc/hexane, 9 : 1), 0.2; ^{1}H NMR (DMSO-d_6, 500 MHz): δ 8.26–8.06 (m, 3H), 7.79–7.78 (m, 1H), 7.26–7.22 (m, 5H), 7.17–7.16 (m, 1H), 7.05–7.04 (m, 1H), 4.57–4.50 (m, 1H), 4.42–4.41 (m, 1H), 4.27–4.25 (m, 3H), 3.42–3.38 (m, 5H), 3.05–3.04 (m, 1H), 2.83–2.82 (m, 1H), 1.94–1.90 (m, 1H), 1.37 (s, 9H), 0.85–0.52 (m, 6H) ppm; ^{13}C NMR (125 MHz, DMSO-d_6): δ 173.0, 172.2, 165.3, 155.2, 129.5 (2C), 128.5 (2C), 126.5, 125.1, 80.5, 54.6 (2C), 40.8, 39.2, 38.6 (3C), 38.2, 37.7 (2C), 28.6 (3C), 19.6, 17.7 ppm; IR (KBr): 3116, 2911, 2102, 1675, 1384, 1276, 915; ^{195}Pt NMR (107 MHz, DMSO-d_6): δ −2960 ppm; HRMS (ESI) exact mass calcd for $C_{26}H_{40}N_{11}O_6$ $[M + H]^+$ 602.3163, found 602.3184.

Pt-Conjugate 26. Yellow solid; yield = 80%; ^{195}Pt NMR (107 MHz, DMSO-d_6): δ −2960 ppm; HRMS (ESI) exact mass calcd for $C_{26}H_{43}Cl_2N_7O_6PtK$ $[M + K]^+$ 853.1937, found 853.1947, *m*/*z* 852, 853, 854, 855, 856, 857.

Tetraazide 31 (precursor of 32a). White solid; R_f (EtOAc/hexane, 7 : 3), 0.3; ^{1}H NMR ($CDCl_3$, 400 MHz): δ 7.58–7.37 (bs, 1H), 7.36–7.28 (bs, 1H), 7.24–7.00 (bs, 1H), 6.40–5.95 (bs, 1H), 4.97–4.74 (bs, 1H), 4.53–4.34 (bs, 2H), 4.24–4.05 (bs, 2H), 3.56–3.37 (m, 8H), 3.16–3.00 (m, 2H), 3.15–3.00 (bs, 1H), 2.55–2.46 (bs, 1H), 1.98–1.78 (m, 1H), 1.73–1.57 (m, 1H), 1.49–1.33 (m, 22H) ppm; ^{13}C NMR ($CDCl_3$, 100 MHz): δ 172.1, 171.8, 171.0, 156.6, 156.0, 80.8, 79.3, 53.3, 51.6, 51.5 (2C), 51.4, 49.0, 48.8, 48.4, 39.9, 37.6, 31.4, 29.6, 28.5 (3C), 28.3 (3C), 22.6 ppm; 3216, 2925, 2102, 1675, 1544; HRMS calculated for $C_{26}H_{45}N_{17}O_7Na$ $[M + Na]^+$ 730.3586, found 730.3596.

Diplatinum conjugate (32a). Colour: brown; yield = 71%; ESI-MS *m*/*z* 1100 $[M - Cl]^+$, isotopic peaks 1096, 1097, 1098, 1099, 1100, 1101, 1102, 1103, 1104, 1105.

Diplatinum conjugate (32b). Yield = quantitative; colour = brown; hygroscopic solid; HRMS (ESI-MS) calculated for $C_{16}H_{38}N_9O_3Cl_4Pt_2$ $[M + H]^+$ 934.1147, found 934.1149, isotopic peaks *m*/*z* 932, 933, 934, 935, 936, 937, 938, 939, 940, 941, 942.

Conflicts of interest

There are no conflicts to declare.

Acknowledgements

Financial support of this work from the Indian Institute of Technology Madras, India (CHY/14-15/831/RFER/KMMU), and SERB, DST (EMR/2016/003973), is gratefully acknowledged. We, in addition, thank the Department of Chemistry and DST (FIST)

facility for instrumentation support. We also thank the Department of Biotechnology, IIT Madras, for support with biological assays. SK thanks IIT Madras, KV thanks CSIR (India) and SS thanks the DST INSPIRE Scheme for their fellowships.

Notes and references

1 A.-M. Florea and D. Buesselberg, *Cancers*, 2011, **3**, 1351–1371.
2 R. A. Alderden, M. D. Hall and T. W. Hambley, *J. Chem. Educ.*, 2006, **83**, 728.
3 Y. Jung and S. J. Lippard, *Chem. Rev.*, 2007, **107**, 1387–1407.
4 C. A. Rabik and M. E. Dolan, *Cancer Treat. Rev.*, 2007, **33**, 9–23.
5 N. J. Wheate, S. Walker, G. E. Craig and R. Oun, *Dalton Trans.*, 2010, **39**, 8113–8127.
6 O. Rixe, W. Ortuzar, M. Alvarez, R. Parker, E. Reed, K. Paull and T. Fojo, *Biochem. Pharmacol.*, 1996, **52**, 1855–1865.
7 U. Ndagi, N. Mhlongo and M. E. Soliman, *Drug Des., Dev. Ther.*, 2017, **11**, 599–616.
8 L. Guo, G. Lv, L. Qiu, H. Yang, L. Zhang, H. Yu, M. Zou and J. Lin, *Eur. J. Pharmacol.*, 2016, **786**, 60–71.
9 P. Zhang and P. J. Sadler, *J. Organomet. Chem.*, 2017, **839**, 5–14.
10 G. Gasser, I. Ott and N. Metzler-Nolte, *J. Med. Chem.*, 2011, **54**, 3–25.
11 C. Yang, W. Wang, G.-D. Li, H.-J. Zhong, Z.-Z. Dong, C.-Y. Wong, D. W. J. Kwong, D.-L. Ma and C.-H. Leung, *Sci. Rep.*, 2017, **7**, 42860.
12 L. Zeng, P. Gupta, Y. Chen, E. Wang, L. Ji, H. Chao and Z.-S. Chen, *Chem. Soc. Rev.*, 2017, **46**, 5771–5804.
13 P. Zhang and P. J. Sadler, *Eur. J. Inorg. Chem.*, 2017, 1541–1548.
14 T. C. Johnstone, K. Suntharalingam and S. J. Lippard, *Chem. Rev.*, 2016, **116**, 3436–3486.
15 S. van Zutphen and J. Reedijk, *Coord. Chem. Rev.*, 2005, **249**, 2845–2853.
16 S. Mukhopadhyay, C. M. Barnes, A. Haskel, S. M. Short, K. R. Barnes and S. J. Lippard, *Bioconjugate Chem.*, 2008, **19**, 39–49.
17 F. Barragán, D. Carrion-Salip, I. Gómez-Pinto, A. González-Cantó, P. J. Sadler, R. de Llorens, V. Moreno, C. González, A. Massaguer and V. Marchán, *Bioconjugate Chem.*, 2012, **23**, 1838–1855.
18 H. M. Coley, J. Sarju and G. Wagner, *J. Med. Chem.*, 2008, **51**, 135–141.
19 Y. Y. Scaffidi-Domianello, K. Meelich, M. A. Jakupec, V. B. Arion, V. Y. Kukushkin, M. Galanski and B. K. Keppler, *Inorg. Chem.*, 2010, **49**, 5669–5678.
20 J. P. Parker, M. Devocelle, M. P. Morgan and C. J. Marmion, *Dalton Trans.*, 2016, **45**, 13038–13041.
21 B. W. Harper, A. M. Krause-Heuer, M. P. Grant, M. Manohar, K. B. Garbutcheon-Singh and J. R. Aldrich-Wright, *Chem. – Eur. J.*, 2010, **16**, 7064–7077.
22 T. Servidei, C. Ferlini, A. Riccardi, D. Meco, G. Scambia, G. Segni, C. Manzotti and R. Riccardi, *Eur. J. Cancer*, 2001, **37**, 930–938.
23 V. Brabec, J. Kašpárková, O. Vrána, O. Nováková, J. W. Cox, Y. Qu and N. Farrell, *Biochemistry*, 1999, **38**, 6781–6790.
24 N. J. Wheate and J. G. Collins, *Coord. Chem. Rev.*, 2003, **241**, 133–145.
25 M. S. Robillard, A. R. P. M. Valentijn, N. J. Meeuwenoord, G. A. van der Marel, J. H. van Boom and J. Reedijk, *Angew. Chem., Int. Ed.*, 2000, **39**, 3096–3099.
26 S. Abramkin, S. M. Valiahdi, M. A. Jakupec, M. Galanski, N. Metzler-Nolte and B. K. Keppler, *Dalton Trans.*, 2012, **41**, 3001–3005.
27 M. W. Ndinguri, R. Solipuram, R. P. Gambrell, S. Aggarwal and R. P. Hammer, *Bioconjugate Chem.*, 2009, **20**, 1869–1878.
28 Y.-H. Chu, M. Sibrian-Vazquez, J. O. Escobedo, A. R. Phillips, D. T. Dickey, Q. Wang, M. Ralle, P. S. Steyger and R. M. Strongin, *Mol. Pharmaceutics*, 2016, **13**, 2677–2682.
29 T. Karasawa, M. Sibrian-Vazquez, R. M. Strongin and P. S. Steyger, *PLoS One*, 2013, **8**, e66220.
30 K. Ramalingam, N. Raju, P. Nanjappan and D. P. Nowotnik, *Tetrahedron*, 1995, **51**, 2875–2894.
31 M. S. Robillard, S. van Alphen, N. J. Meeuwenoord, B. A. J. Jansen, G. A. van der Marel, J. H. van Boom and J. Reedijk, *New J. Chem.*, 2005, **29**, 220–225.
32 R. Wirth, J. D. White, A. D. Moghaddam, A. L. Ginzburg, L. N. Zakharov, M. M. Haley and V. J. DeRose, *J. Am. Chem. Soc.*, 2015, **137**, 15169–15175.
33 M. S. Robillard, A. R. P. M. Valentijn, N. J. Meeuwenoord, G. A. Van der Marel, J. H. Van Boom and J. Reedijk, *Angew. Chem., Int. Ed.*, 2000, **39**, 3096–3099.
34 M. Bodanszky and S. Natarajan, *J. Org. Chem.*, 1975, **40**, 2495–2499.
35 P. Moutevelis-Minakakis, C. Sinanoglou, V. Loukas and G. Kokotos, *Synthesis*, 2005, 933–938.
36 R. Krikavova, J. Vanco, T. Silha, J. Marek and Z. Travnicek, *J. Coord. Chem.*, 2016, **69**, 2422–2436.
37 J. Zhao, W. Li, R. Ma, S. Chen, S. Ren and T. Jiang, *Int. J. Mol. Sci.*, 2013, **14**, 16851–16865.
38 C. Icsel, V. T. Yilmaz, Y. Kaya, H. Samli, W. T. A. Harrison and O. Buyukgungor, *Dalton Trans.*, 2015, **44**, 6880–6895.
39 R. F. Pasternack, M. Caccam, B. Keogh, T. A. Stephenson, A. P. Williams and E. J. Gibbs, *J. Am. Chem. Soc.*, 1991, **113**, 6835–6840.
40 B. C. Baguley and M. Le Bret, *Biochemistry*, 1984, **23**, 937–943.
41 M. Kantoury, M. Eslami Moghadam, A. A. Tarlani and A. Divsalar, *Chem. Biol. Drug Des.*, 2016, **88**, 76–87.
42 J. Marmur, *J. Mol. Biol.*, 1961, **3**, 208–218.
43 M. E. Reichmann, S. A. Rice, C. A. Thomas and P. Doty, *J. Am. Chem. Soc.*, 1954, **76**, 3047–3053.
44 N. Shahabadi and L. Heidari, *Spectrochim. Acta, Part A*, 2014, **128**, 377–385.
45 R. C. Borra, M. A. Lotufo, S. M. Gagioti, F. D. M. Barros and P. M. Andrade, *Braz. Oral Res.*, 2009, **23**, 255–262.
46 W. A. G. W. N. Hafiza and S. Y. Latifah, *OncoTargets Ther.*, 2014, **7**, 1375–1387.